ORIGINAL PAPER

Modelling garnet-fluid partitioning in H₂O-bearing systems: a preliminary statistical attempt to extend the crystal lattice-strain theory to hydrous systems

Amit Meltzer[1] · Ronit Kessel[1]

Abstract

Accurate geochemical models of magmatic processes require an understanding of crystal-melt partitioning of trace elements. Many major igneous processes at different tectonic environments in Earth occur in the presence of garnet as a residual phase. Since the pioneering crystal lattice-strain model, several attempts have been made to quantify garnet-melt partitioning coefficients over a wide range of conditions. However, high pressure high-temperature experimental data demonstrate distinct differences in partitioning determined at anhydrous conditions and partitioning determined in the presence of H₂O. In this study, we present for the first time a constraint on the partitioning of REE, Y, and Sc between garnet and hydrous fluids as a function of the water content in the fluid phase. We analysed published hydrous experimental partitioning data using different statistical methods and modelled key parameters in the crystal lattice strain model (r_0, D_0, and E). We show a robust correlation between r_0, temperature and garnet-fluid partitioning of Mg. We further show that D_0 can be predicted using the garnet-fluid partitioning of Fe and that E can be predicted using various parameters describing the fluid phase. We validate and illustrate the ability to predict partitioning of REE in H₂O-bearing systems using major element analysis of garnet and fluid only. Consequently, our statistical model paves the way to integrate thermodynamic models based on major element chemical equilibria with trace element studies on hydrous magmatic systems, allowing a description of the transfer of key trace elements in more realistic conditions.

Keywords REE · Partitioning coefficients · Crystal lattice strain model · HP-HT experiments · Fluid-rock interaction

Introduction

Understanding magmatic processes within the inaccessible Earth, such as deep partial melting and crystallization, can be derived from trace element and isotope geochemistry (Allegre and Minster 1978; Gast 1968; Neumann et al. 1954; Shaw 1953; Zou and Reid 2001). Trace elements have no direct control on the formation or consumption of major

✉ Amit Meltzer
  Amit.Meltzer@mail.huji.ac.il

[1] Institute of Earth Sciences, The Hebrew University of Jerusalem, 91904 Jerusalem, Israel

phases, due to the negligible influence of trace elements on the composition and stability of the major phases. However, their passive nature and widely varying physical and chemical properties make them very sensitive trackers of rock history and evolution (Blundy and Wood 1994; Goldschmidt 1937; Shaw 1953). To decipher the evolution of a given magmatic rock, one needs to know the high-pressure high-temperature (HP-HT) characteristics of trace elements during melting and crystallization. The reliability of the conclusions depends on our ability to accurately predict the correct affinity of trace elements during a given process.

The partitioning of trace elements between a mineral and a fluid phase (we refer to a fluid phase as a general term for any mobile phase in equilibrium with the mineral assemblage) is described by a partition coefficient (labelled here as D). Following the Nernst equation, a partition coefficient is defined as the concentration ratio of a given element between the mineral and the fluid [following the terminology of Beattie et al. (1993)]. It is well established that partition

coefficients are a complex function of pressure, temperature, oxygen fugacity, phase stability, and bulk composition (Blundy and Wood 1994, 2003a, b; Gaetani et al. 2003; Hertogen and Gijbels 1976; Mysen 2004; Prowatke and Klemme 2005; van Westrenen et al. 2000b; Wood and Blundy 2002).

Blundy and Wood (1994) developed the crystal lattice-strain model, that provided an elementary framework for quantifying variations in D. This model builds upon the observation, first made by Onuma et al. (1968), that a near-parabolic dependence of mineral-melt partition coefficients, D_i, exists as a function of trace element radius, r_i, for a series of isovalent elements i substituting onto a particular crystal lattice site. The crystal lattice-strain model is based on three parameters describing the variations in D_i for an isovalent set of elements: (1) r_0—the 'ideal radius' for a (fictive) element with charge $j+$ that minimally strains the crystal lattice and hence has the largest mineral-melt D_i; (2) D_0—the maximum partition coefficient for this 'ideally sized' trace element; (3) E—the apparent Young's modulus of the site, which is a measure for the resistance of the crystal lattice to the incorporation of an element with different radius than the ideal radius, r_0. The relation between these three parameters and the observed values of D_i and r_i for the set of elements is presented in Eq. (1), taken from Blundy and Wood (1994)

$$D_i = D_0 * \exp\left[\frac{-4\pi * E * N_A\left(\frac{r_0}{2}(r_i - r_0)^2 + \frac{1}{3}(r_i - r_0)^3\right)}{RT}\right] \tag{1}$$

where R is the gas constant, T is the temperature (Kelvin), and N_A is Avogadro's number. The model provides a quantitative thermodynamic expression relating the variation in partition coefficients, and the physical properties of the host crystal as a function of ionic radii. By fitting this equation to a determined set of D_i's, one can calculate r_0, D_0, and E of the lattice site at the given conditions. Knowledge of these parameters as a function of P, T, and bulk composition allows one to quantify the behaviour of individual trace elements at these conditions even in cases where they are not measured.

A significant number of studies focused on the behaviour of rare earth elements (REE, also called the lanthanides) and Y, all predominantly in the $+3$ oxidation state under common mantle conditions. REE are preferentially incorporated into garnet and clinopyroxene in terrestrial mantle lithologies. Therefore, knowledge of the partition coefficients of REE between these two minerals and a fluid phase is important to interpret melting and crystallization processes in various settings in the upper mantle. The trivalent REE and Y have radii in the range of 1.001 and 1.172 Å in the VIII-fold coordination (Shannon 1976). They are similar in radii to the divalent cations Mg^{2+}, Fe^{2+} and Ca^{2+} occupying the dodecahedral X-site in garnet [0.89, 0.92 and 1.12 Å in VIII-fold coordination (Shannon 1976), respectively]. Thus, REE and Y are believed to substitute into the X-site of the garnet, with coupled substitution required for charge balance (Quartieri et al. 1999a, b, 2002, 2004; van Westrenen et al. 1999). The substitution of Sc, also a trivalent ion, into the various structural sites of the garnet is still controversial. The models of van Westrenen et al. (1999), Corgne and Wood (2004), Draper and van Westrenen (2007), van Westrenen and Draper (2007), Westrenen et al. (2001), and Wood and Blundy (2002) all treated Sc as a trivalent element entering the X-site of the garnet, as later ratified in the studies of Oberti et al. (2006) and Kim et al. (2007). In contrast, Sun and Liang (2013) claimed that Sc enters both the X as well as the Y sites in garnet. To avoid uncertainties in the potential errors in the determination of the partitioning of Sc into the X-site of the garnet, they modelled the partitioning only of REE and Y between garnet and anhydrous melts.

Since the pioneering work of Blundy and Wood (1994), many studies (e.g. Draper and van Westrenen 2007; van Westrenen et al. 1999, 2000a, b, 2001, 2003; van Westrenen and Draper 2007) used additional experimental data on REE, Y and Sc partitioning at a wide P–T conditions in a variety of bulk anhydrous mantle lithologies to fit r_0, D_0 and E values and parameterized these values as a function of pressure, temperature and major element garnet composition.

Although partition coefficients are a function of both crystal and melt compositions and structures, only the dependence on the garnet composition was thoroughly demonstrated. van Westrenen et al. (1999), van Westrenen et al. (2000b) and others showed that the relative compatibility of trace elements in anhydrous systems is dominated by the structure of the crystal. For example, changes in the garnet composition reflect changes in its crystal structure, affecting the energetics of substituting a trace cation for an essential structural constituent. These studies further showed that r_0 for REE increases while D_0 decreases with increasing Mg/(Mg+Ca) ratio in the garnet. With increasing garnet Fe content (the almandine fraction), D_0 value decreases. The influence of the melt phase composition was represented only by the partitioning of major elements: D_{Mg} in the statistical model of Draper and van Westrenen (2007) or D_{Fe} in the thermodynamic model of van Westrenen and Draper (2007).

The anhydrous crystal lattice-strain model was successfully used to provide a quantitative understanding of magmatic processes beneath mid-ocean ridges (Frey et al. 2011), at the source of hot spots (Corgne et al. 2012; Howarth et al. 2014) as well as on extra-terrestrial planets (Draper et al. 2006; Papike et al. 2013; Van Kan Parker et al. 2011). However, many deep Earth processes, such as dehydration and hydrous melting in subduction zones as well as metasomatism beneath subcontinental lithospheres, involve volatiles, mainly H_2O. Despite the importance of water in igneous

processes, there is only a limited number of studies focusing on trace element partitioning in hydrous systems (Ayers et al. 1997; Brenan et al. 1995a, b, 1998; Brenan and Watson 1991; Gaetani et al. 2003; Kessel et al. 2005a, 2015a; Mysen 2004; Tatsumi et al. 1986). The scarcity of data is due to many experimental and analytical challenges in deriving the compositions of aqueous fluids and hydrous melts in equilibrium with mantle lithologies at HP-HT conditions.

Wood and Blundy (2002) used available experimental data at the time in an attempt to apply the crystal-lattice strain model, that originally developed for anhydrous systems, to hydrous environments. They fitted REE partition coefficients between garnet or clinopyroxene and hydrous melts and showed that the D_0 values predicted from the anhydrous model were highly overestimated compared to the fitted values. They empirically updated the crystal lattice-strain model to incorporate the effect of H_2O in the melt on partition coefficients. Due to the limited set of data on hydrous systems at the time, their model was calibrated to melts with up to 45 wt% H_2O in equilibrium with clinopyroxene and melts with up to 24 wt% H_2O in equilibrium with garnet.

Lastly, Sun and Liang (2013) fitted REE and Y partitioning data in olivine, clinopyroxene and garnet from anhydrous experiments and calibrated expressions for the three lattice strain parameters. Based on their anhydrous model, they explored the effect of water on the partition coefficients, using published data from hydrous experiments. They concluded that even though their empirical garnet-melt partitioning model was calibrated on anhydrous garnet-melt data, it can also reproduce partition coefficients for the hydrous experiments very well.

Despite the progress made by Wood and Blundy (2002) and Sun and Liang (2013), the effect of melt composition, especially in hydrous systems, on trace element partitioning, remains unclear. For example, Kessel et al. (2005a) determined partition coefficients between eclogite and water-rich fluids and melts containing H_2O in the range of 10–90 wt% at 4–6 GPa and temperatures of 700–1200 °C. The experimentally fitted D_0 between eclogitic garnet and an aqueous fluid containing 83 wt% H_2O at 4 GPa and 800 °C was found to be ~600. The predicted value following the anhydrous model of van Westrenen and Draper (2007) is $9.2*10^4$ (3 orders of magnitude higher) and following the anhydrous model of Sun and Liang (2013) is ~18 (an order of magnitude lower). The predicted value following the hydrous model of Wood and Blundy (2002) is 1940. This value is one order of magnitude lower than the predicted value using the anhydrous model but is still overestimated compared to the fitted value for D_0. When the experimental partitioning results are compared with existing crystal lattice-strain models (both anhydrous and hydrous), it is apparent that these discrepancies cannot be reconciled by considering only the composition of the garnet. The available experimental

studies on hydrous systems clearly show that melt composition, especially the H_2O content in the fluid phase, is an important factor in element compatibility in the mantle. Although Wood and Blundy (2002)'s model improved our ability to predict partition coefficients in hydrous environments, its applicability to many settings in the deep Earth remains limited, and the effect of volatiles in the fluid over a wide range of compositions, pressures and temperatures is still severely under-constrained.

We compiled the available experimental data on REE, Y and Sc partitioning between garnet and H_2O-bearing fluid in hydrous systems at mantle conditions. In the absence of systematic partitioning data as a function of pressure, temperature and bulk composition, a thermodynamic based crystal-chemical model cannot be developed at this stage. We approached the data from a statistical perspective, similar to the approach taken by Draper and van Westrenen (2007), and tried to predict how REE partitioning into mantle garnet is affected by the presence of H_2O-bearing fluids. We assume that Sc enters the X-site of the garnet, following the approach taken by van Westrenen et al. (1999) and subsequent papers mentioned above, and obtained best-fit values for the three crystal lattice-strain model's parameters (r_0, D_0, E) for hydrous HP-HT experiments. The fitted values were used in multiple linear regressions relating sixteen variables that reflect the possible influence of mineral composition and stoichiometry, melt composition and structure, major-element partitioning, pressure, temperature and water content. The model for r_0, D_0 and E presented in this study, allows one to predict the partitioning of REE, Y and Sc between garnet and hydrous fluid at pressures of 1.5–7.5 GPa and temperatures of 700–1230 °C.

Methods

In this section, we present the data sources used in our analysis, layout the assumptions for our error calculation, and outline the compositional variables used for the statistical evaluation. The fitting process and all the statistical calculations were performed using various Matlab functions.

The database

Mantle garnets are mainly divided into two groups, peridotitic and eclogitic. Shown in Fig. 1 are the compositional fields of anhydrous eclogitic and peridotitic garnets as compiled by Mottana (1986) and van Westrenen et al. (2000b). Eclogitic garnets are Cr-poor, Ca-rich pyrope-grossular-almandine mixtures with wide variations in the grossular content. Peridotitic garnets are composed of about 75% pyrope, 10% grossular and 15% almandine. These garnets are rich in Cr and Fe^{3+}. Superimposed
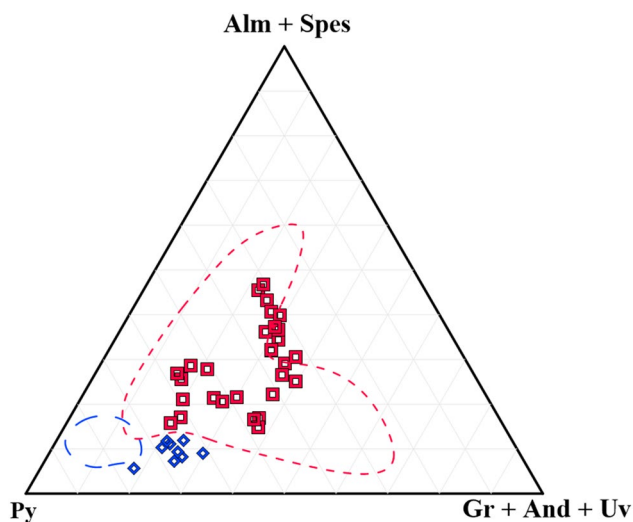
Fig. 1 Literature compilation of experimental garnet compositions in mantle lithologies in equilibrium with H_2O-bearing fluids. Red—eclogitic garnets, blue—peridotitic garnets. Superimposed on this triangle are the compositional fields found for anhydrous mantle garnets as complied by Mottana (1986) and van Westrenen et al. (2000a, b). *Py* pyrope ($Mg_3Al_2Si_3O_{12}$), *Alm* almandine ($Fe_3Al_2Si_3O_{12}$), *Spes* Spessartine ($Mn_3Al_2Si_3O_{12}$), *Gr* grossular ($Ca_3Al_2Si_3O_{12}$), *And* andradite ($Ca_3Fe_2Si_3O_{12}$), *Uv* uvarovite ($Ca_3Cr_2Si_3O_{12}$)

on these fields, are the experimental garnet compositions found in hydrous systems as compiled in this study (Tables 1, 2). Hydrous eclogitic garnets have similar compositions to anhydrous eclogitic mantle garnets. The experimental hydrous peridotitic garnets are slightly richer in grossular and andradite components compared to anhydrous peridotitic garnets.

Despite the importance of HP-HT experimental studies focusing on garnet-fluid partitioning of REE in hydrous systems, there are only a limited number of such scope. Most of these studies inferred the fluid composition from mass balance constraints or by examining quench precipitates in between minerals. Kessel et al. (2005b, 2015b) used the diamond aggregates method to trap fluids within their interstices, allowing a more direct approach in determining fluid composition for a wide range of P–T conditions. However, both indirect and direct approaches encounter measurement uncertainties, especially in HREE contents in the fluid phase due to their high incompatibility.

Several studies focused on partition coefficients of trace elements between eclogite and H_2O-bearing fluids (Tables 1, 2). Kessel et al. (2005a) studied the interaction of H_2O-bearing fluids with K-free eclogite at 4–6 GPa and temperatures of 700–1200 °C. They found the solidus at 4 GPa to be between 850 and 900 °C and at 5 GPa between 1000 and 1050 °C. Subsolidus fluids contained up to ~90 wt% H_2O and supersolidus melts contained 15–35 wt% H_2O. The system at 6 GPa was found to be above the second critical end-point and a supercritical fluid with H_2O content between 10 and 80 wt% is stable at temperatures between 800 and 1200 °C. Adam and Green (2006) performed experiments at 3.5 GPa and 1180–1190 °C, where an eclogitic garnet is in equilibrium with a hydrous melt containing 13–15 wt% H_2O. Klimm et al. (2008) studied trace element partitioning between eclogite and H_2O-fluids at 2.5 GPa and 750–900 °C. Based on textures of quench solute, they concluded that the fluid was supercritical and estimated the amount of water in the fluid, but only the exsolved quench glass fraction was analysed. Green et al. (2000), Barth et al. (2002) and Gaetani et al. (2003), studied trace element partitioning between

Table 1 List of Sc-bearing experiments used to fit r_0, E, D_0 and to statistically evaluate r_0

Reference	Number of experiments	Pressure (GPa)	Temperature (°C)	Bulk composition	H_2O in fluid phase[a] (wt%)
Kessel et al. (2005a)	14	4–6	700–1200	K-free MORB	30–87
Adam and Green (2006)	2	3.5	1180, 1190	Basanite	13–15

[a]A fluid phase is used as a general term for any mobile phase in equilibrium with a mineral assemblage

Table 2 List of Sc-absent experiments used to statistically evaluate E, D_0

Reference	Number of experiments	Pressure (GPa)	Temperature (°C)	Bulk composition	H_2O in fluid phase[a] (wt%)
Green et al. (2000)	7	3–7.5	1100–1200	Tholeiitic basanite	10–39
Barth et al. (2002)	4	1.8	1000, 1040	Tonalite	6–9
Gaetani et al. (2003)	1	1.6	1230	Natural basalt	6
Kessel et al. (2015a)	6	4–6	1000–1200	K-bearing lherzolite	23–66

[a]A fluid phase is used as a general term for any mobile phase in equilibrium with a mineral assemblage

eclogitic garnets and hydrous melts with water contents between 6 and 39 wt%. Klein et al. (2000) experimentally determined partition coefficients between 1–3 GPa and temperatures of 900–1150 °C. They doped the starting material with trace element oxides in concentrations of 0.5 wt% each. No more than two trace element oxides were added to one experimental charge to minimize changes in bulk composition and to avoid mutual analytical interferences.

Kessel et al. (2015a) is the only study, known to us, which determined REE partitioning between peridotitic garnet and H_2O-bearing fluid. They studied the interaction of H_2O-bearing fluids with K-bearing peridotites at 4–6 GPa and temperatures of 1000–1200 °C. They found the solidus at 4 GPa to be between 900 and 1000 °C and at 5–6 GPa between 1100 and 1200 °C. Subsolidus fluids contained up to ~ 80 wt% H_2O and supersolidus melts contained 20–40 wt% H_2O.

Scandium is an essential element in fitting the REE partition coefficients between garnet and a fluid phase to Onuma's parabola. van Westrenen et al. (1999) and van Westrenen et al. (2000b) have shown that mantle garnets in anhydrous systems partition trivalent elements into the X-site such that r_0 values are in the range of 0.91–0.93 Å. Therefore, all REE are on the right limb of Onuma's parabola. One of the fundamental assumptions of Onuma's parabola is that the elastic strain energy is roughly symmetrical around the optimum ion (r_0, D_0). This is an important assumption, especially when one considers partitioning of REE into garnet, as all REE are larger than the mentioned range of r_0. Scandium, with a radius of 0.885 Å, is the only trivalent trace element with radius lower than r_0. Fitting the data from Sc-bearing experiments allows us to best fit the partition coefficient data to Onuma parabola's using Eq. (1), providing fitted values of r_0, D_0, and E. These three values are referred hereinafter as the fit parameters. In the absence of Sc partition coefficient, the left-hand limb of the Onuma parabola for trivalent elements is unconstrained. Although, fitting partitioning data without Sc to Eq. (1) is possible, this method yields fit parameters that are physically unrealistic—e.g. generally low r_0, low E and consequently high D_0. The misfit of the left-hand limb of the Onuma parabola was described in length in Draper and van Westrenen (2007) and in van Westrenen et al. (2000b). Thus, in this study, data from Sc-absent experiments were fitted to Eq. (1) only after constraining one of the fit parameters. This approach was taken in previous models of garnet-melt partitioning (van Westrenen et al. 2000b; van Westrenen and Draper 2007) and zircon-melt partitioning of REE, which suffers from the same problem (Hanchar and Van Westrenen 2007). Accordingly, we separated the published experimental partitioning data in hydrous systems into two groups—Sc-bearing experiments (Table 1) and the other Sc-absent experiments

(Table 2). Following this approach, the Sc-bearing experiments were used to predict r_0 values for the Sc-absent experiments to fit D_0 and E to the measured experimental partitioning data.

Some of the possible partitioning data were excluded from different steps of the calibration process of the model. All the partitioning data from Klimm et al. (2008) were excluded. In their study, glasses were characterized by very low MgO content, in the order of 0.01–0.12 wt%, significantly outside the range of MgO content found in all other reported experiments in Tables 1, 2. In addition, the REE content in the glasses is low compared to other experiments, with high uncertainties (up to 50%), leading to very high partition coefficients between garnet and fluid with large uncertainties. For example, the partition coefficient of Lu between garnet and fluid at 800 °C is 1277 ± 584. This partition coefficient is higher than any partition coefficient of Lu found in the literature in hydrous systems. These observations would greatly influence the uncertainties in the model calibration, thus were excluded. Kessel et al. (2005b) determined the second critical end-point between 5 and 6 GPa. The partitioning coefficients at 6 GPa were fitted to Eq. (1) but were not used in the calibration of the three fit parameters, as further explained in the following sections. The data from Klein et al. (2000) were also excluded from the fitting process due to the different doping quantities of the trace elements and to the fact that not all REE were present in a singular experiment. This study was used to validate the model.

r_0, D_0 and E fitting

The experimental REE, Y, and Sc partitioning data from the references given in Table 1, were fitted to Eq. (1) using the Levenberg–Marquardt nonlinear least-squares algorithm, yielding values for all three fit parameters for each experiment. To take into account the measurement uncertainties in the fitting process, for each element the algorithm randomly picks a D_i value within the measured 1σ error margins of the measured D, constructing a new D dataset for each experiment. It then fits this new dataset to Eq. (1). Performing 10,000 runs of this Monte Carlo calculation for a given experiment, we found the median value and its uncertainties for each of the fit parameters. The uncertainties on fit parameters are presented by the 84.13th and 15.87th percentile values (corresponding to 1σ in a normal distribution). An example of this approach is presented in Fig. 2, showing the experimental D_i vs. ionic radius, r_i for the REE, Y and Sc entering the garnet X-site in equilibrium with an aqueous fluid containing 83 wt% H_2O at 4 GPa and 800 °C (Kessel et al. 2005a). Superimposed on the data is the fitted curve for the measured D_is, the median calculated curve considering
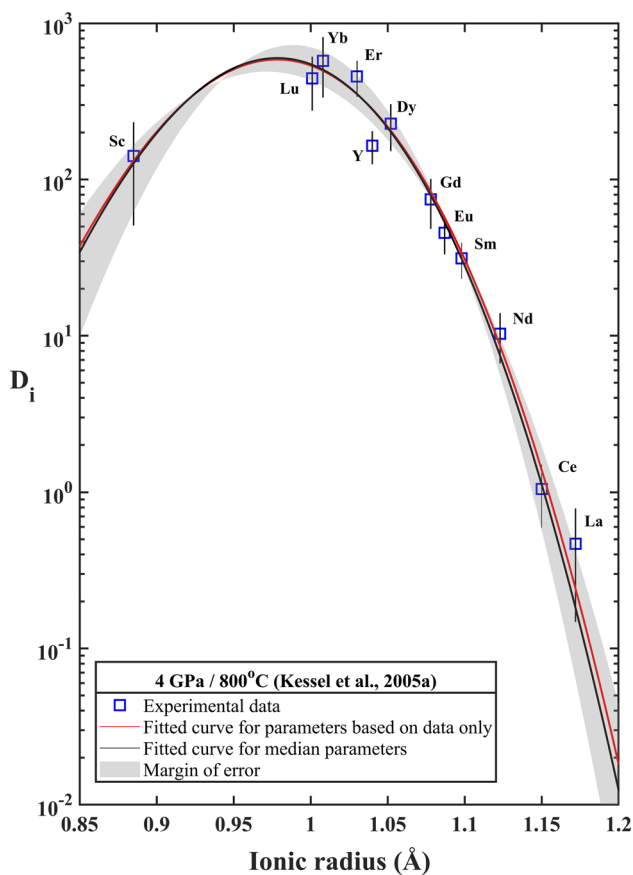
Fig. 2 An example of measured partition coefficients for trivalent elements (REE, Y and Sc) between eclogitic garnet and aqueous fluid containing 83 wt% H_2O at 4 GPa and 800 °C from Kessel et al. (2005a) as a function of ionic radii (Shannon 1976). Uncertainties are 1 standard deviation on the average values. The elements show a parabolic behavior. Superimposed on the data are fit curves of Eq. (1). The red curve is the fit to the data ignoring uncertainties. The black solid curve is the fit to the data for the median parameters (see text). The grey strip is the margin of error represented by the area enclosed between two curves using the positive and negative errors of each fit parameter

the measurement uncertainties on D_is, and the error margin curves using the error on the median fit parameters.

Parameterization of r_0, D_0 and E

From the three fit parameters for the Sc-bearing experiments, r_0 values showed the most limited range of values. Therefore, our strategy was to use a modelled r_0 value as a constraint to fit Eq. (1) to the Sc-absent experiments. The fitted r_0 values of the Sc-bearing experiments (Table 1) were modelled following the statistical approach taken by Draper and van Westrenen (2007). We selected sixteen variables intended to reflect garnet and fluid compositions (Table 3): contents of the major endmember components (pyrope, grossular, and almandine) to reflect the variation in garnet compositions; D values for Ca, Mg, and Fe (the major constituent cations for the garnet X-site) and K_D values for both Fe–Mg and Al–Si exchange to reflect garnet-fluid major element equilibrium; FeO/SiO_2, MgO/SiO_2 ratios, and Mg# in the fluid phase to reflect the variation in the melt compositions. Similar variables were used in Draper and van Westrenen (2007). We added the mole fraction of water in the fluid phase to these variables. In experiments where the water content in the fluid phase was not reported, the total amount of water (in wt%) was calculated from subtracting the total amount of oxides from 100. The mole fraction of water was calculated out of the reported fluid composition. All parameters were calculated on a hydrous basis and used the wt% values.

Possible bivariate correlations among the set of variables were assessed to find combinations in which variables were independent of one another. This was accomplished by computing correlation matrices consisting of Pearson's correlation coefficients with their associated p-values for all possible variable pairs for the entire database (Supplementary Table S1). For example, temperature and water fraction in

Table 3 Variables chosen for possible use in statistical regression

Variable	Description
D_{Ca}, D_{Mg}, D_{Fe}	Garnet-fluid D values for major constituents of X-site $\left[\frac{oxide_{garnet}(wt\%)}{oxide_{fluid}(wt\%)} \right]$
K_D for Fe–Mg, Al–Si	$K_D^{Fe-Mg} = \frac{FeO^{grt}*MgO^{liq}}{FeO^{liq}*MgO^{grt}}$; $K_D^{Al-Si} = \frac{Al_2O_3^{grt}*SiO_2^{liq}}{Al_2O_3^{liq}*SiO_2^{grt}}$ [a]
Mol% Gr, Py, Alm	Mol% grossular, pyrope, almandine in garnet
Si, Al per formula unit (apfu)	Number of Si and Al cations per 12-oxygen formula unit
Fluid Mg#	$Mg/(Mg+Fe)_{molar}$ in fluid
$(MgO/SiO_2)_{fluid}$	MgO/SiO_2 (wt%) in fluid
$(FeO/SiO_2)_{fluid}$	FeO/SiO_2 (wt%) in fluid
Fluid χ_{H_2O}	Molar H_2O/all oxides in fluid
10,000/T	Kelvin
P	GPa

[a]All oxide values are in wt%; grt and liq refer to contents in coexisting garnet and liquid, respectively

the fluid are strongly correlated in these experiments, thus are difficult to separate.

The values of r_0 were multiply regressed against combinations of these independent variables. Due to the limited set of data, only 2 predicting variables were included to avoid overfitting. A stepwise approach was taken, allowing us to determine which of the predicting variables were truly required. We weighted the significance of each of the coefficients determined by the regression using an F-statistic test. Parameters with F-values smaller than 0.6 were considered insignificant.

The multiple linear regression of r_0 was used to calculate r_0 values for the Sc-absent experiments (Table 2). These calculated r_0 values were then implemented as a constraint in Eq. (1) to fit values for D_0 and E following the same Monte Carlo calculation algorithm explained above. We then modelled the resulting D_0 and E values derived for all experiments (Tables 1, 2) using the sixteen possible predicting variables mentioned above in separated multiple linear regressions.

Results

Fit parameters' models

The multiple linear regressions found to best predict r_0, D_0, and E are shown in Table 4. A full comparison between this study's fitted and modelled parameters and corresponding modelled fit parameters from other studies is provided in Supplementary Table S2. In the following sections, we examine the results for each of the parameters in detail and discuss them in comparison to the previously existing models (Sun and Liang 2013; van Westrenen and Draper 2007; Wood and Blundy 2002).

r_0 model

The fitted r_0 values found for Sc-bearing experiments are between 0.946 and 0.992 Å and are shown in Fig. 3 as a function of the fraction of H_2O in the fluid phase (χ_{H_2O}). At

Table 4 Coefficients of multiple linear regressions performed on subsets of variables

Fit parameters	Regression variables	R^2 values
r_0[a]	T, D_{Mg}	0.969
D_0[b]	D_{Fe}	0.839
E	FeO/SiO$_2$, χ_{H_2O}, Fluid Mg#	0.544

[a]The regression was performed using only the Sc-bearing experimental data (Table 1)

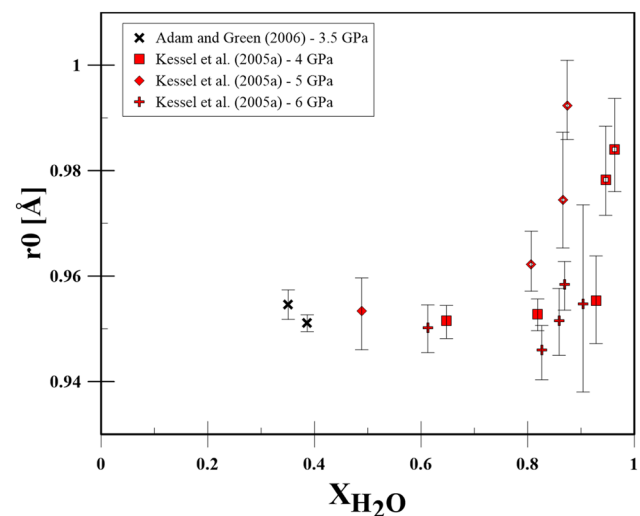[b]The regression was performed using all the data set (Tables 1, 2)

Fig. 3 Fitted values of r_0 for REE as function of the fraction of H_2O in the fluid phase for Sc-bearing experiments (Table 1). Filled symbols indicate experiments containing mantle garnets in equilibrium with hydrous melts. Open symbols indicate experiments containing mantle garnets in equilibrium with aqueous fluids. Experiments at 6 GPa Kessel et al. (2005a) are beyond the second critical endpoint of the system as determined in Kessel et al. (2005b)

pressures between 3.5 and 5 GPa, the r_0 values for supersolidus garnets in equilibrium with hydrous melts are relatively constant, between 0.951–0.955 Å, regardless of the H_2O content in the melt or the pressure. By contrast, the r_0 values for subsolidus garnets in equilibrium with aqueous fluids increase with increasing H_2O content in the fluid. The r_0 values for eclogitic garnets at 6 GPa in equilibrium with a supercritical fluid are 0.946–0.958 Å, within the range of r_0 values found in supersolidus experiments, regardless of the water content in the supercritical fluid (ranging from 30 to 72 wt%). As suggested by Kessel et al. (2005a), the supercritical fluid demonstrated more melt-like properties, that consequently influenced the partitioning.

As mentioned above, we multiply regressed the fitted r_0 values found for the Sc-bearing experiments, excluding the r_0 values of the supercritical fluid from Kessel et al. (2005a), as further discussed in the next section. To avoid overfitting of the data and to reduce the degrees of freedom we used only two variables each time and assumed no interactions between them. From the 121 possible variable combinations, only five generated R^2 values above 0.9, and included only T or 10,000/T, D_{Mg} or MgO/SiO$_2$, D_{Ca}.

Because the r_0 parametrisation is needed as a constraint to fit the partitioning data of the Sc-absent experiments to Eq. (1), we decided to further evaluate only variable combinations that show similar ranges for the Sc-bearing and Sc-absent experiments (Tables 1, 2). For example, the average value of D_{Mg} of the Sc-bearing experiments is 9.259 ± 8.04 (1 SD). The D_{Mg} values of all 24 Sc-absent

experiments are within this range. On the contrary, the mol% Gr value of only five Sc-absent experiments is within the range of mol% Gr in the Sc-bearing experiments. The only variables that fulfilled the criterion of similar values within all experiments, were T or 10,000/T, D_{Mg} or MgO/SiO_2, D_{Ca}, and χ_{H_2O}. The most successful model (highest R^2) out of the five combinations predicting r_0 as a function of different variables is given in Eq. (2):

$$r_0(REE, Å) = 1.083(\pm0.009) - 9.027 * 10^{-5}(\pm6.005 * 10^{-6}) * T \\ -7.865 * 10^{-4}(\pm1.449 * 10^{-4}) * D_{Mg}$$

(2)

Errors are standard errors on the coefficients, and the variables are further explained above and in Table 3. The predicted r_0 values for the Sc-bearing experiments compared to the fitted values are shown in Fig. 4. Equation (2) predicts r_0 to within ±0.009 Å (1σ), slightly better than the ±0.017 Å found for anhydrous systems by van Westrenen and Draper (2007). The accuracy in the prediction of both models is less than the difference in ionic radius between most adjacent REE.

As detailed above, most garnet-fluid partitioning studies did not include Sc (Table 2). Equation (2) provides a way to predict r_0 for the REE partitioning between garnet and fluid. The r_0 values calculated for the Sc-abse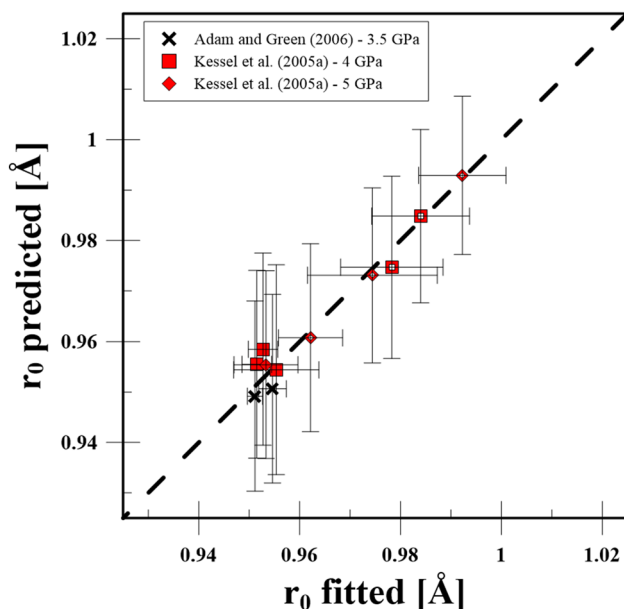nt experiments are in the range of 0.946–0.973 Å, similar in range to the r_0 values found for Sc-bearing experiments. A similar trend to that shown in Fig. 3 is observed in the r_0 values predicted for the Sc-absent experiments. The predicted r_0 values increase with increasing water content in the fluid phase, both for eclogitic garnets as well as peridotitic garnets.

Wood and Blundy (2002) followed the conclusion of van Westrenen et al. (2000b) that although r_0 values vary with melt composition and structure, the effect of water on r_0 is insignificant. Therefore, they did not incorporate an equation for calculating r_0 in hydrous systems. Calculating r_0 values for all hydrous experiments using van Westrenen and Draper (2007) anhydrous model results in values of 0.8808–0.9336 Å, much smaller than the fitted values found for these experiments [the predicted values of r_0, D_0 and E following the anhydrous model of van Westrenen and Draper (2007) are also given in Supplementary Table S2 next to fitted and modelled values of this study]. The deviation of our predicted r_0 values from the r_0 calculated using van Westrenen and Draper (2007)'s model increases with increasing χ_{H_2O}, from 2 to 11% deviation, both for eclogitic as well as peridotitic garnets. The calculated r_0 values for all hydrous experiments using Sun and Liang (2013) equation (Eq. 11 in their paper) are between 0.8343 and 1.0235 Å. These calculated values either underestimate or overestimate our fitted values to all experiments compiled in this study (Supplementary Table S3).

The fitted and modelled r_0 values of hydrous experiments used in this study (Tables 1, 2) demonstrate that the fluid's nature and water content have a major effect on partitioning in garnets in H_2O-bearing systems. Our hydrous model predicts an increase in r_0 values with increasing water content in the fluid phase, and consequently a decrease in r_0 values with increasing temperature, an opposite trend compared to van Westrenen and Draper (2007) and Draper and van Westrenen (2007) which assumed thermal expansion in their anhydrous models. Furthermore, our hydrous model suggests that the intrinsic effect of crystallographic site expansion with temperature increase is overwhelmed by the effect of the structure of the fluid. It further confirms that r_0 is not merely crystallography-based parameter but rather is influenced by the presence and structure of coexisting fluid, as previously suggested by van Westrenen et al. (2000a).

D_0 model

The predicted r_0 values for the Sc-absent experiments were used to fit the partitioning data to Eq. (1) and find D_0. Shown in Fig. 5 are the fitted D_0 values for both the Sc-bearing and Sc-absent experiments, as a function of water content in the fluid phase. D_0 values vary by over 2 orders of magnitude, ranging from 1 to 600—a far greater spread than seen in anhydrous data. The uncertainties shown in Fig. 5 are the
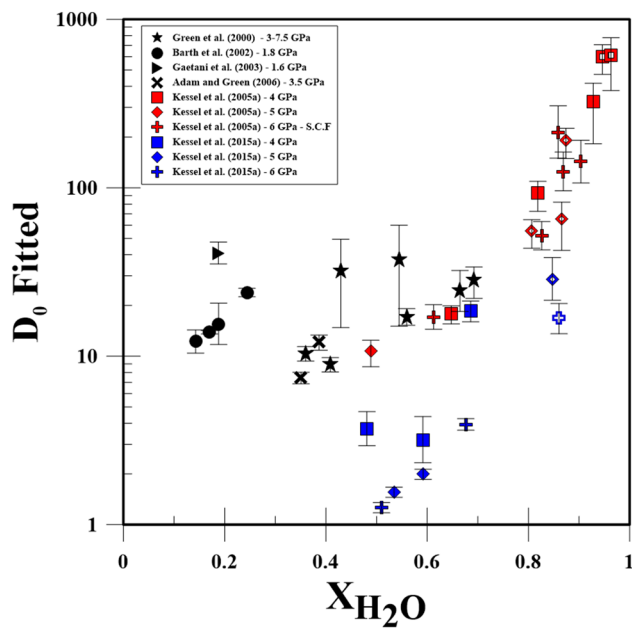

Fig. 4 Comparison between predicted and fitted values of r_0 for REE partitioning between mantle garnets and H_2O-bearing fluids for Sc-bearing experiments (Table 1). Symbols are identical to those in Fig. 3. Uncertainties on the fitted values are the 15.87th and the 84.13th percentile values and on the predicted values are 1 standard error on the parameters from Eq. 2 (see text for further explanation). The dashed line is a 1:1 line

Fig. 5 Fitted values of D_0 for REE as function of the fraction of H_2O in the fluid phase for all experiments (Tables 1, 2). Symbols are identical to those in Fig. 3

84.13th and 15.87th percentiles, calculated using the same procedure as described in the methods section. The D_0 values of supersolidus peridotitic garnets are between 1 and 10. The D_0 values for the subsolidus peridotitic garnets is ~ 20. The D_0 values for eclogitic garnets are higher than those for the peridotitic garnets at similar water content in the fluid. The D_0 values in supersolidus eclogitic garnets in equilibrium with hydrous melts are between 10 and 40, regardless of the water content in the melt or the pressure. The D_0 values sharply increase up to 600 with increasing H_2O content in the fluid phase, regardless of the pressure.

The D_0 values of eclogitic garnets in equilibrium with supercritical fluids at 6 GPa demonstrate a similar trend to that observed at lower pressures. Although the r_0 values of these experiments were similar to those determined for supersolidus experiments, i.e. suggesting a melt-like behaviour, the D_0 values continue the fluid to melt trend as seen at 4–5 GPa, i.e. suggesting a fluid-like behaviour. Due to the limited number of experiments to test the consistency of the decoupling between the trends of r_0 and D_0 values and the water content at supercritical conditions, we decided to exclude the available partitioning data of Kessel et al. (2005a) experiments conducted at 6 GPa from the linear regressions of the different fit parameters. Furthermore, the effect of water on the garnet-supercritical fluid partitioning is beyond the scope of this study.

We multiply regressed the fitted D_0 values from all the experimental database (Sc-bearing and Sc-absent experiments). Similar to the modelling process for r_0, we limited

the search to 2 parameters each time to avoid overfitting of the data. The regressions with the highest correlation were the ones using D_{Fe} as one variable, paired with either P, K_D^{Al-Si}, Fluid Mg#, or $[MgO/SiO_2]_{fluid}$. Including an additional variable to D_{Fe} was greatly below the threshold of 0.6 in the F-statistic test, with or without assuming an intercept in the regression. This suggests that the only significant parameter influencing the prediction of D_0 is D_{Fe}. The resulting prediction of D_0, based on all the experiments, is given in Eq. (3) (errors are 1 standard error):

$$D_0 = 7.2(\pm 0.5) * D_{Fe} \qquad (3)$$

The next step in validating our D_0 model was to assess the regression in a 'leave-one-out' cross-validation process. The aim of the cross-validation process was to evaluate if and how a specific experiment influences the regression, i.e. the coefficients used for each predictive parameter and the coefficients of determination (R^2). The only experiment that influenced the R^2 of the regression was RK201 [eclogitic garnet in equilibrium with aqueous fluid at 4 GPa and 700 °C, taken from Kessel et al. (2005a)]. Excluding this experiment didn't change the regression coefficient of D_{Fe}, supporting the consistency of the model. However, it improved the regression prediction, increasing R^2 value from 0.84 to 0.96, verifying the major influence of this specific experiment on the regression and the mismatch of the predicted D_0 value for this experiment.

The predicted D_0 values for all experiments compared with the fitted values are shown in Fig. 6. The average relative deviation of the model D_0 from the fitted values for all experiments is 128%. For the 28 eclogitic experiments, 50% of the eclogitic D_0 values are predicted to within 50% deviation and 67% of the experiments are predicted to within 80% deviation. The relatively high uncertainties in predicting D_0 are a result of the incorporation of propagated uncertainties in the D_i values. Difficulties in determining the trace element compositions in the fluid led to high uncertainties in D_i.

The anhydrous model for D_0 of van Westrenen et al. (2001) used D_{Mg}. The latest improved thermodynamic model for D_0 of van Westrenen and Draper (2007) used D_{Fe} term. Anhydrous eclogitic garnets in the van Westrenen and Draper (2007) compilation are characterized by relatively high D_{Fe} and high D_0. Anhydrous peridotitic garnets (majorities) have much lower D_{Fe} and D_0. Similar correlation between D_{Fe} and D_0 is seen in the hydrous systems, the eclogitic garnets are characterized by higher D_0 values compared to peridotitic garnets at a given water content in the fluid phase. The D_{Fe} values are highly correlated with fluid χ_{H_2O} values, as indicated by the low p-value of the Pearson's correlation coefficients (Supplementary Table S1).

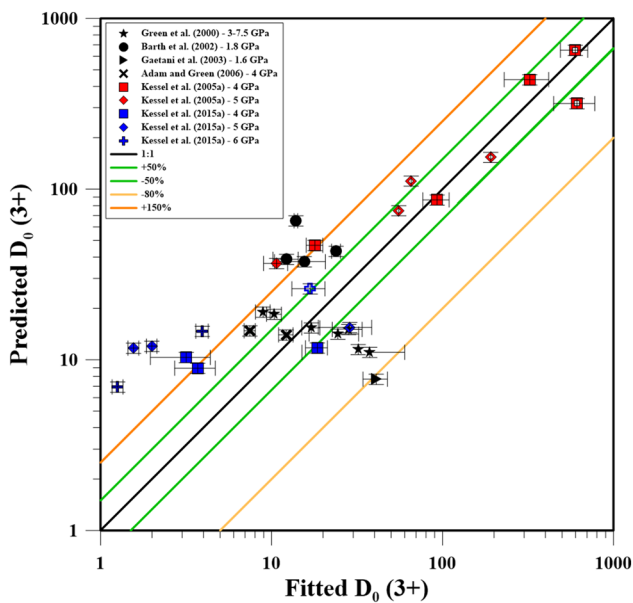Wood and Blundy (2002) showed that the D_0 values for REE in hydrous systems are 2–4 orders of magnitude lower

Fig. 6 Comparison between predicted and fitted values of D_0 for REE partitioning between mantle garnets and H_2O-bearing fluids for experiments in Tables 1, 2. Symbols are similar to those in Fig. 3. Uncertainties on the fitted values are the 15.87th and the 84.13th percentile values and on the predicted values are 1 standard error on the parameters from Eq. 3 (see text for further explanation). The black line is a 1:1 line. Also shown are lines representing uncertainties in the order of 50, 80 and 150%

Fig. 7 Fitted values of E for REE as function of the fraction of H_2O in the fluid phase for all experiments (Tables 1, 2). Symbols are identical to those in Fig. 3

than based on predictions from anhydrous systems. As shown in Supplementary Table S2, the predicted D_0 values for all the hydrous experiments in Tables 1, 2 following the model of Wood and Blundy (2002) are indeed lower by up to one order of magnitude than those predicted by the anhydrous model of van Westrenen and Draper (2007), but still 2 orders of magnitude higher than those found by fitting D_0 to the experimental data. Similar to the prediction of r_0 by Sun and Liang (2013), their D_0 values poorly predict the fitted values in hydrous experiments. For example, their predicted D_{Lu} values are limited to the range between 5 and 200 (Fig. 1 in the Supplementary Table S3) while the measured D_{Lu} values reach lower and higher values.

E model

Fitted E values for all experiments listed in Tables 1, 2 range mostly from 287 to 742 GPa, with two experiments having E values of 944 and 1110 GPa. The fitted E values as a function of χ_{H_2O} in the fluid phase are shown in Fig. 7. For comparison, the range of E values for the trivalent trace elements entering the garnet X-site in anhydrous systems is 465–730 GPa (van Westrenen and Draper 2007). The E values for garnets in hydrous systems are larger in range than the values for garnets in anhydrous systems. We multiply
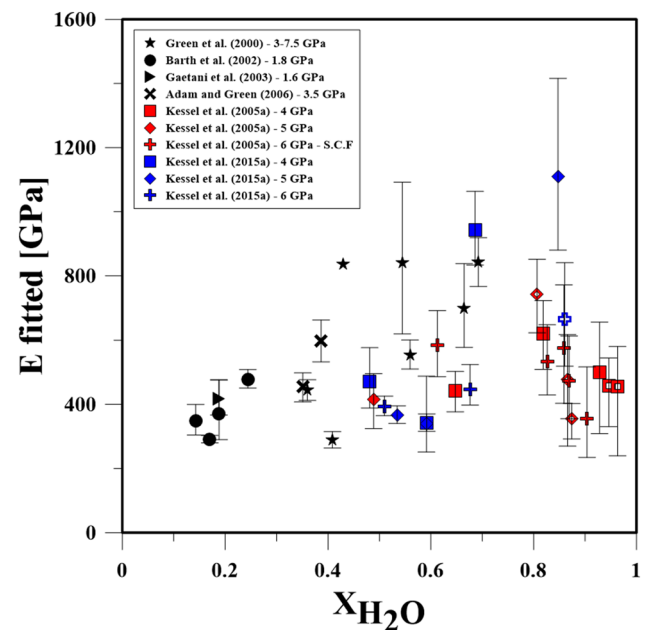
regressed the fitted E values, this time expanding the search to 3 parameters, to try covering the entire range of values. The resulting model predicting E is given in Eq. (4) (errors are 1 standard error):

$$E(GPa) = 485(\pm 135) + 1854(\pm 375) * \left[Feo/SiO_2\right]_{fluid}$$
$$- 542(\pm 211) * Mg\#_{fluid} + 350(\pm 111) * \chi_{H_2O}$$
$$(4)$$

The predicted E values compared to the fitted values are shown in Fig. 8. Even though the R^2 value is relatively low (0.54), Eq. (4) predicts E for all experiments in Tables 1, 2 to within 85 GPa (1σ). This value is close to the average standard deviation for fitted values of E (80 GPa, 1σ) for anhydrous systems in van Westrenen and Draper (2007).

Discussion

The new hydrous model and comparison to previous models

Equations (2–4) provide new parametrizations for the three crystal-lattice strain model fit parameters r_0, D_0, and E, for the compatibility of trivalent elements (REE, Y and Sc) in garnet in equilibrium with H_2O-bearing fluids. These
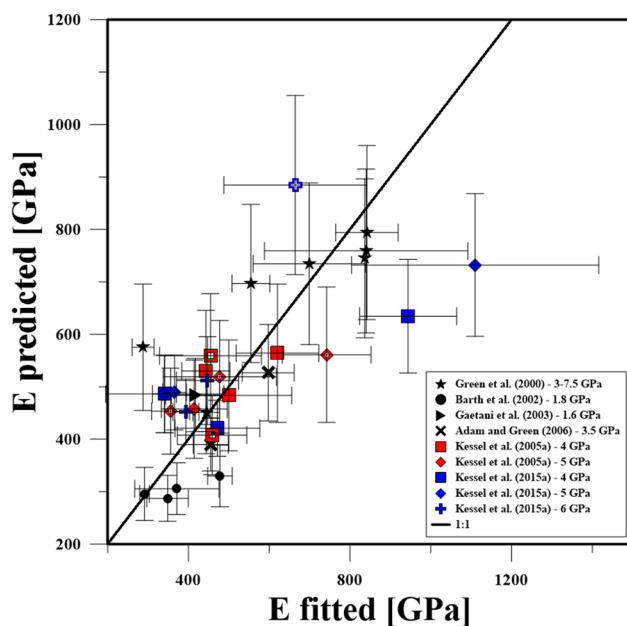
Fig. 8 Comparison between predicted and fitted values of E for REE partitioning between mantle garnets and H_2O-bearing fluids for experiments in Tables 1, 2. Symbols are identical to those in Fig. 3. The black line is a 1:1 line

parameterizations are based on a limited set of inputs: the major element compositions of garnet and fluid at a given temperature and pressure.

In Fig. 9, we compare measured D_i values with those predicted from our model, as well as those predicted by previous models. In Fig. 9a we plot partitioning data from a subsolidus experiment of eclogite in equilibrium with H_2O-bearing fluid containing 83 wt% H_2O at 800 °C and 4 GPa (Kessel et al. 2005a). Figure 9b shows the partitioning data from the same study, slightly above the solidus, at 1000 °C. The hydrous melt in this experiment contains 56 wt% H_2O. Both datasets were included in our statistical database. The measured partition coefficients included REE, Y and Sc, allowing us to fit all three parameters (r_0, D_0 and E) to the measured D_is. Our fit, as well as our predicted curves (black and green, respectively), are shown in both figures. Our new model does an excellent job in predicting the experimental measurements. As expected, the anhydrous model of van Westrenen and Draper (2007) predicts lower r_0 and significantly higher D_0 values than fitted (dashed orange). We followed the suggestion of van Westrenen et al. (2000a), calculated r_0 values for all experiments in the database using the model of van Westrenen and Draper (2007), and fitted D_0 and E to the measured D_i values. The r_0 values predicted from this anhydrous model are significantly lower than the fitted r_0 values by this study, resulting in a mismatch of the Onuma parabola for most REE (dotted orange).

Even though Sun and Liang (2013) based their model on different assumptions, we used their predicting expressions for the three fit parameters (Eqs. 10–12 in their study) to plot and compare their model with the model presented in this study and the measured hydrous partitioning data. As can be seen in Fig. 9 (dashed red), their model underestimates the measured values of the subsolidus experiment (Fig. 9a) and overestimates the measured values of HREE of the supersolidus experiment (Fig. 9b). Lastly, we used our fitted r_0 and E values and calculated D_0 values using the hydrous model of Wood and Blundy (2002). The D_0 values predicted by Wood and Blundy (2002) constitute a substantial improvement over the different anhydrous models but still cannot predict the measured partitioning coefficients for most hydrous experiments (dashed blue).

Model validation: comparison between the new hydrous model and measurements

Most experimental or natural sample studies report only the major element composition of the garnet and/or the fluid phase. Trace element compositions are either completely missing or available for only one of the phases (garnet in most cases), thus no partition coefficients are available. If the temperature of equilibrium between the garnet and fluid is known (in the experiment) or assumed/calculated (for natural samples), using the hydrous model presented in this study we are able to calculate D_i values for all REE according to the following procedure:

(a) We use the garnet and fluid major element compositions in each experiment at a given pressure and temperature to calculate r_0, D_0 and E [using Eqs. (2, 3 and 4), respectively].

(b) We then use Eq. (1) and the values of r_0, D_0 and E to calculate the D_i values of all REE given their radius r_i.

An example of such a procedure is given using the study of Klein et al. (2000), which as mentioned above was not part of our model's calibration. Klein et al. (2000) experimentally determined the partitioning of REE and HFSE (high field strength elements) between garnets and andesitic to granodioritic melts (containing 5–15 wt% H_2O) at a pressure of 1.5 GPa at temperatures of 900, 1000 and 1150 °C. At each pressure and temperature, 6–7 separate experiments were performed, each experiment doped with only two trace elements.

To test our model, we used the major element compositions of the garnet and fluid phases and calculated the fit parameters to calculate individual elemental partition coefficients. Then, we compared them to the measured values.

The percent relative mismatch between model predictions (based on major element compositions of the phases) and
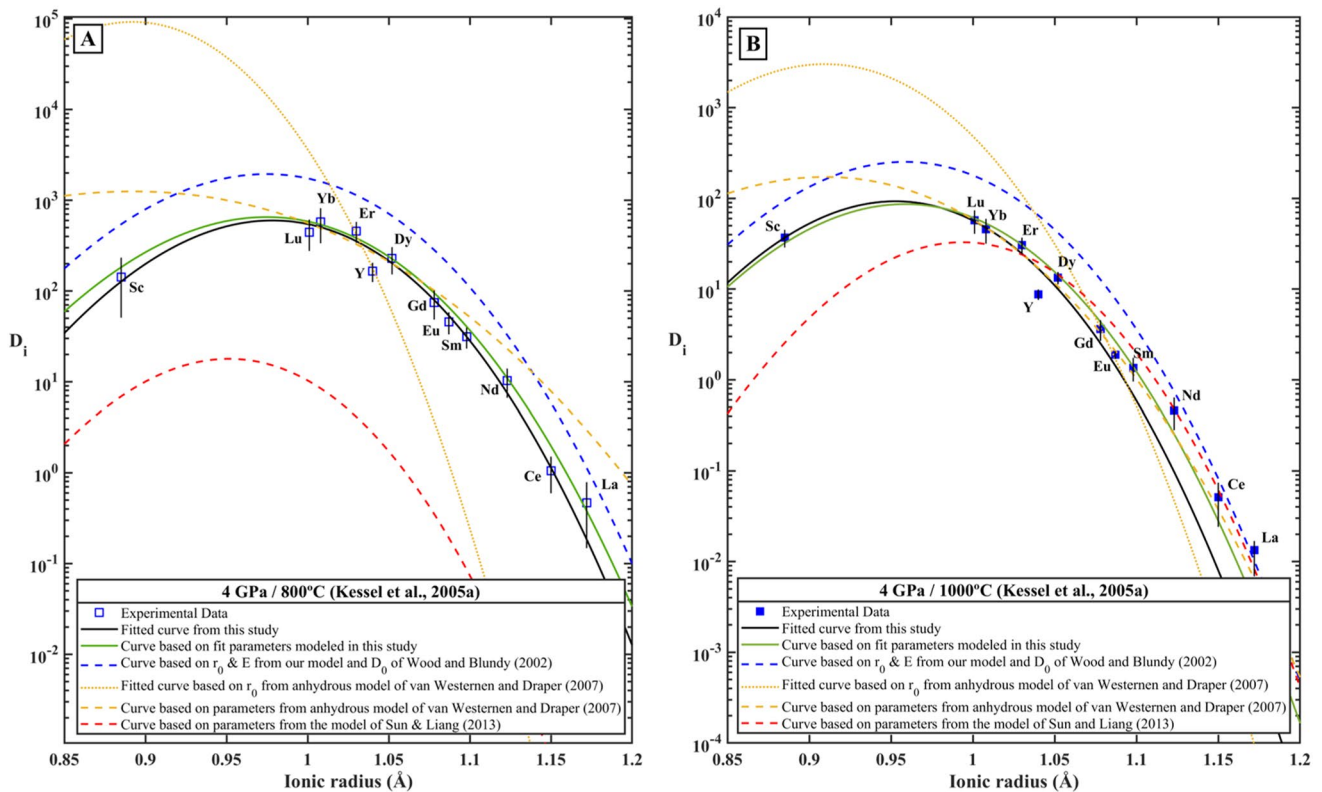
Fig. 9 Comparison between different models predicting the fit parameters. Symbols are similar to those in Fig. 3. The green and black lines are the fitted and modeled fit parameters (respectively) from this study. The dotted orange curve is based on the fit parameters reported in van Westrenen and Draper (2007). The dotted orange curve is based on the fitting procedure to a r_0 constrain calculated using van Westrenen and Draper (2007). The dashed blue curve is based on the r_0 and E calculated using Eqs. 2 and 4, and D_0 calculated using Wood and Blundy (2002). See text for further explanation

Table 5 Relative mismatches between measured and predicted values of garnet-melt partition coefficients from Klein et al. (2000)

Mismatch (%)	La	Ce	Nd	Sm	Eu	Gd	Dy	Er	Yb	Lu
900 °C	73	179	333	95	314	186	212	28	97	150
1050 °C	84	598	661	110	201	67	373	4	29	12
1100 °C	40	145	158	153	20	41	204	6	30	26
Average	65	307	384	120	178	98	263	9	52	62

measurements of each element in each set of experiments at a given pressure and temperature as reported in Klein et al. (2000) is listed in Table 5. The predicted D_i values are shown in Fig. 10 compared with the measured values. The D_i values for the HREE are identical within uncertainties (taking into consideration both experimental uncertainties and the uncertainties derived from our model). The mismatch in predicting D_i values for the LREE is high and reaches 600% relative. Because of the high incompatibility of these elements and high measurements uncertainties of their analysis in the garnet phase, LREE is difficult to work within partitioning studies and display significant mismatches when modelling their partitioning (Draper and van Westrenen 2007; van Westrenen and Draper 2007).

Possible explanations for the 'water effect'

Despite the preliminary stage of this model and our limited understanding of the statistical correlation to the physical properties, we offer some potential reasons to the major effect of water content in the fluid phase on trace element partitioning. Several studies suggested that increase in the degree of polymerization of the melt can increase trace element partitioning coefficients (Ellison and Hess 1990, 1994; Evans et al. 2008; Gaetani 2004; Gaetani et al. 2003; Huang et al. 2006; Mysen 2004; Ryerson and Hess 1978). While Gaetani et al. (2003) and Gaetani (2004) concluded that addition of water decreases the degree of melt polymerization and may lead to a decrease in REE partitioning
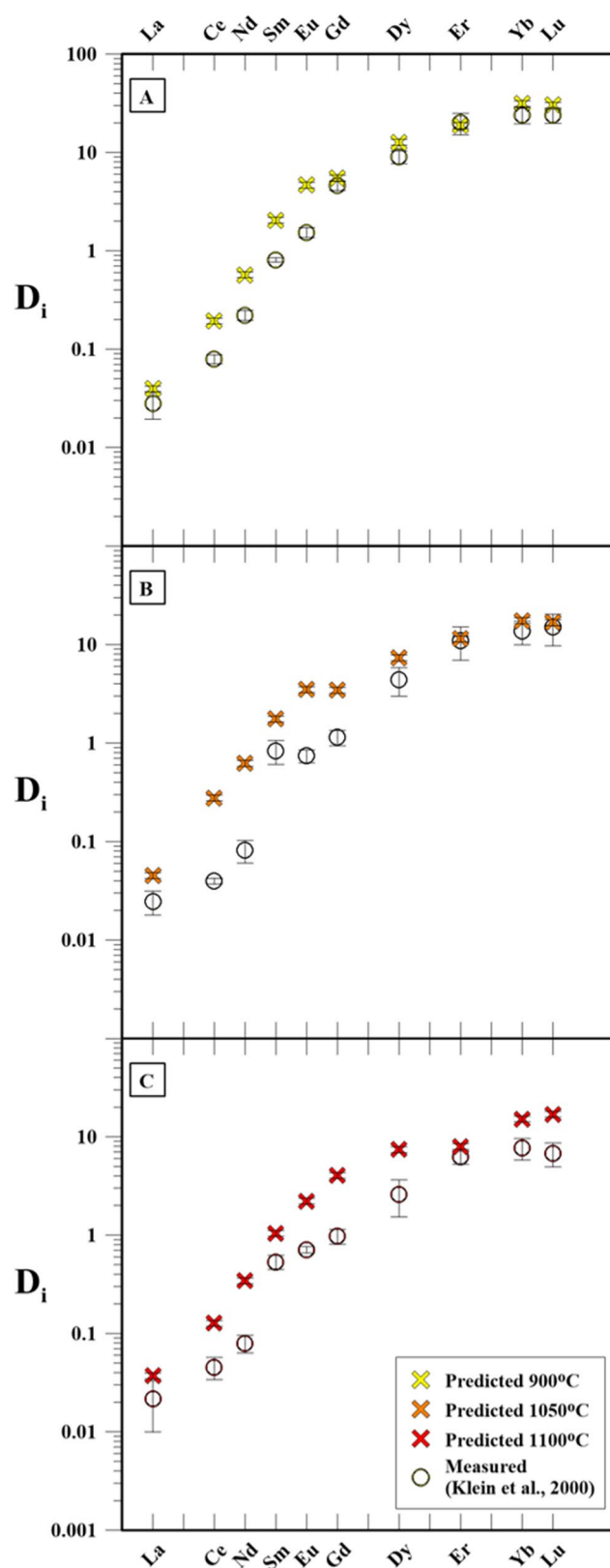
Fig. 10 Comparison between this study predicted values and measured values of REE partitioning from Klein et al. (2000). Uncertainties on the measured values are calculated using customary error estimation. The uncertainties on the predicted values are 1 standard error on the parameters from Eq. (2, 3, 4)

coefficient values, the trends presented above suggest otherwise. We suggest that the influence of the degree of polymerization shows indirect effect in hydrous systems or is overridden by other primary melt structure properties.

Other studies proposed complexation in silicate melts [review in Hess (1995)] to explain variations of partitioning coefficients. The conclusion of O'Neill and Eggins (2002) that REE form very stable oxides, led Prowatke and Klemme (2005) to offer this formation as a support to the existence of REE-alumino-silicate complexes in silicate melts. Other experimental studies on mineral solubilities and trace elements partitioning in HP-HT fluids (Antignano and Manning 2008; Audétat and Keppler 2005; Hayden and Manning 2011; Louvel et al. 2013; Wilke et al. 2012) explained the enhancement of trace element mobility by the enrichment of major element solutes in the fluid, especially those that form alkali-alumino-silicate complexes (e.g. HFSE). Huang and Sverjensky (2019) modelled the metal-silicate complexes of fluids reported in Kessel et al. (2005b) and Kessel et al. (2015b) used in this study's database. They concluded that at upper mantle conditions in Cl-free fluids, the Al-bisilicate complex $[Al(OH)_3OSi(OH)_3^-]$ becomes the most important Al-complex. They reported the strong temperature dependence and the increase in this complex concentration with increasing temperature.

Another possible explanation for the major effect of water on trace element partitioning can be attributed to the differences in coordination of trace elements in melts and minerals. Ponader and Brown Jr (1989) reported changes in the REE coordination due to changes in melt composition. They concluded that an increase in irregularity in the coordination leads to an increase in REE activity in polymerized melts which could, in turn, cause an increase of crystal-melt partition coefficients. van Westrenen et al. (2000a) showed that r_0 and E values could be influenced by large variations in the local melt coordination environment of REE, Y and Sc, which may be a result of the presence of significant amounts of water. At this stage, with the currently limited data on REE solubility and activities in silicate melts and fluids, we are not yet in a position to fully understand and quantify what the influence of water is on the structural properties of these melts or fluids.

Future developments

In their concluding remarks, Blundy and Wood (2003b) identified three possible future developments in studying trace elements partitioning: computer simulation in different aspects of partitioning calculation and modelling; spectroscopic studies of trace species and their behaviour; trace element partitioning between minerals and aqueous fluids over a wide range of conditions. A significant progress has been made in recent years in experimental and analytical

determination of major as well as trace element compositions of fluids in equilibrium with mantle lithology. Based on these studies it was made possible to develop a preliminary model for the behaviour of REE, Y and Sc in hydrous mantle environment. Nevertheless, there is a crucial need for more consistent experimental partitioning data of trace elements, including Sc and HFSE, in various conditions of the upper mantle in equilibrium with various volatiles. Despite the advancements made by Kessel et al. (2005a) and Kessel et al. (2015a), a wide range of conditions (P, T, bulk mantle lithology, fO_2, volatiles) is not yet explored. For example, there is no experimental study known to us that measured trace element partitioning in the presence of both H_2O and CO_2 as well as investigating the role of fO_2 on partitioning. Moreover, only recently, some progress has been made in experimental solubility measurements of major and trace elements in Cl^--bearing hydrous systems (Chu et al. 2011; Safonov and Butvina 2013; Tsay et al. 2014, 2016, 2017). However, these experiments are yet to cover the temperature and pressure conditions of the mantle.

Looking back at the three parallel future developments offered by Blundy and Wood (2003b), we suggest pursuing an integrative approach in the study of trace element partitioning. Experimental solubility measurements of trace elements must be used in the development of the up-to-date thermodynamic model. Detailed information on trace species in their crystal-lattice environment from ongoing high energy X-ray studies, must be cross-checked with molecular modelling of trace complexation in fluids and atomistic simulation of trace elements incorporating into minerals using computer modelling. The integration of experimental, analytical and modelling research approaches will advance our understanding of trace element mobility and provide key insights to the role of their exchange between different geodynamic environments.

Conclusions

Predictive models of mineral-melt partition coefficients are required to accurately evaluate processes such as melting, crystallization and metasomatism. The crystal lattice strain model was developed for anhydrous systems, showing that the bulk compositional effect of the crystal is dominant over those of the melt. However, the various anhydrous models were shown to overestimate partition coefficients for hydrous systems. The current study demonstrates that the chemical and structural effect of the silicate hydrous fluids, especially the water content in the fluid phase, on partition coefficients can be significant. The systematic relationship between the mismatch in the anhydrous model r_0 and D_0 values compared to the fitted values and the fluid composition (as demonstrated by the water content in the fluid) suggests that the fluid–structure is influencing partitioning in a manner not accounted for in the existing crystal lattice-strain model.

Here we provide a new predictive model for REE partitioning between garnet and H_2O-bearing fluids with up to 90 wt% H_2O, at pressures between 1.5 and 7.5 GPa and temperatures between 700 and 1230 °C. The model consists of new expressions for r_0, D_0 and E, derived based on statistical considerations. We find that the value of r_0, ~ 0.95 Å, is relatively constant for garnet in equilibrium with hydrous melts. However, r_0 values increase dramatically in garnets in equilibrium with aqueous fluids. D_0 values gradually increase with increasing water content in the fluid phase. We show a significant improvement over the previous models in attempting to quantify REE, Y and Sc partitioning in hydrous systems. However, there are numerous future steps that are needed to be taken to achieve a more accurate model predicting petrogenesis in varying geological environments.

References

Adam J, Green T (2006) Trace element partitioning between mica- and amphibole-bearing garnet lherzolite and hydrous basanitic melt: 1. Experimental results and the investigation of controls on partitioning behaviour. Contrib Miner Petrol 152:1–17. https://doi.org/10.1007/s00410-006-0085-4

Allegre C, Minster J (1978) Quantitative models of trace element behavior in magmatic processes. Earth Planet Sci Lett 38:1–25

Antignano A, Manning CE (2008) Rutile solubility in H_2O, H_2O–SiO_2, and H_2O–$NaAlSi_3O_8$ fluids at 0.7–2.0 GPa and 700–1000 C: implications for mobility of nominally insoluble elements. Chem Geol 255:283–293

Audétat A, Keppler H (2005) Solubility of rutile in subduction zone fluids, as determined by experiments in the hydrothermal diamond anvil cell. Earth Planet Sci Lett 232:393–402

Ayers JC, Dittmer SK, Layne GD (1997) Partitioning of elements between peridotite and H_2O at 2.0–3.0 GPa and 900–1100 C, and application to models of subduction zone processes. Earth Planet Sci Lett 150:381–398

Barth MG, Foley SF, Horn I (2002) Partial melting in Archean subduction zones: constraints from experimentally determined trace element partition coefficients between eclogitic minerals and tonalitic melts under upper mantle conditions. Precamb Res 113:323–340

Beattie P et al (1993) Terminology for trace-element partitioning. Geochim Cosmochim Acta 57:1605–1606

Blundy J, Wood B (1994) Prediction of crystal–melt partition coefficients from elastic moduli. Nature 372:452

Blundy J, Wood B (2003a) Mineral-melt partitioning of uranium, thorium and their daughters. Rev Min 52:59–123

Blundy J, Wood B (2003b) Partitioning of trace elements between crystals and melts. Earth Planet Sci Lett 210:383–397

Brenan JM, Watson EB (1991) Partitioning of trace elements between olivine and aqueous fluids at highP-T conditions: implications for the effect of fluid composition on trace-element transport. Earth Planet Sci Lett 107:672–688

Brenan J, Shaw H, Ryerson F, Phinney D (1995a) Experimental determination of trace-element partitioning between pargasite and a synthetic hydrous andesitic melt. Earth Planet Sci Lett 135:1–11

Brenan J, Shaw H, Ryerson F, Phinney D (1995b) Mineral-aqueous fluid partitioning of trace elements at 900 C and 2.0 GPa: constraints on the trace element chemistry of mantle and deep crustal fluids. Geochim Cosmochim Acta 59:3331–3350

Brenan JM, Ryerson FJ, Shaw HF (1998) The role of aqueous fluids in the slab-to-mantle transfer of boron, beryllium, and lithium during subduction: experiments and models. Geochim Cosmochim Acta 62:3337–3347

Chu L, Enggist A, Luth RW (2011) Effect of KCl on melting in the Mg_2SiO_4–$MgSiO_3$–H_2O system at 5 GPa. Contrib Miner Petrol 162:565–571

Corgne A, Wood BJ (2004) Trace element partitioning between majoritic garnet and silicate melt at 25 GPa. Phys Earth Planet Inter 143:407–419

Corgne A, Armstrong LS, Keshav S, Fei Y, McDonough WF, Minarik WG, Moreno K (2012) Trace element partitioning between majoritic garnet and silicate melt at 10–17 GPa: implications for deep mantle processes. Lithos 148:128–141

Draper DS, van Westrenen W (2007) Quantifying garnet-melt trace element partitioning using lattice-strain theory: assessment of statistically significant controls and a new predictive model. Contrib Miner Petrol 154:731–746

Draper DS, Andrew duFrane S, Shearer CK, Dwarzski RE, Agee CB (2006) High-pressure phase equilibria and element partitioning experiments on Apollo 15 green C picritic glass: implications for the role of garnet in the deep lunar interior. Geochim Cosmochim Acta 70:2400–2416

Ellison AJ, Hess PC (1990) Lanthanides in silicate glasses: a vibrational spectroscopic study. J Geophys Res Solid Earth 95:15717–15726

Ellison AJ, Hess PC (1994) Raman study of potassium silicate glasses containing Rb^+, Sr^{2+}, Y^{3+} and Zr^{4+}: implications for cation solution mechanisms in multicomponent silicate liquids. Geochim Cosmochim Acta 58:1877–1887

Evans TM, O'Neill HSC, Tuff J (2008) The influence of melt composition on the partitioning of REEs, Y, Sc, Zr and Al between forsterite and melt in the system CMAS. Geochim Cosmochim Acta 72:5708–5721

Frey F, Pringle M, Meleney P, Huang S, Piotrowski A (2011) Diverse mantle sources for Ninetyeast Ridge magmatism: geochemical constraints from basaltic glasses. Earth Planet Sci Lett 303:215–224

Gaetani GA (2004) The influence of melt structure on trace element partitioning near the peridotite solidus. Contrib Miner Petrol 147:511–527

Gaetani GA, Kent AJR, Grove TL, Hutcheon ID, Stolper EM (2003) Mineral/melt partitioning of trace elements during hydrous peridotite partial melting. Contrib Miner Petrol 145:391–405. https://doi.org/10.1007/s00410-003-0447-0

Gast PW (1968) Trace element fractionation and the origin of tholeiitic and alkaline magma types. Geochim Cosmochim Acta 32:1057–1086

Goldschmidt VM (1937) The principles of distribution of chemical elements in minerals and rocks. The seventh Hugo Müller Lecture, delivered before the Chemical Society on March 17th, 1937. J Chem Soc 655–673

Green T, Blundy J, Adam J, Yaxley G (2000) SIMS determination of trace element partition coefficients between garnet, clinopyroxene

and hydrous basaltic liquids at 2–7.5 GPa and 1080–1200 C. Lithos 53:165–187

Hanchar JM, Van Westrenen W (2007) Rare earth element behavior in zircon-melt systems. Elements 3:37–42

Hayden LA, Manning CE (2011) Rutile solubility in supercritical $NaAlSi_3O_8$–H_2O fluids. Chem Geol 284:74–81

Hertogen J, Gijbels R (1976) Calculation of trace element fractionation during partial melting. Geochim Cosmochim Acta 40:313–322

Hess PC (1995) Thermodynamic mixing properties and the structure of silicate melts. Struct Dyn Prop Silic Melts 32:145–189

Howarth GH et al (2014) Superplume metasomatism: evidence from Siberian mantle xenoliths. Lithos 184:209–224

Huang F, Sverjensky DA (2019) Extended Deep Earth Water Model for predicting major element mantle metasomatism. Geochim Cosmochim Acta 254:192–230

Huang F, Lundstrom C, McDonough W (2006) Effect of melt structure on trace-element partitioning between clinopyroxene and silicic, alkaline, aluminous melts. Am Miner 91:1385–1400

Kessel R, Schmidt MW, Ulmer P, Pettke T (2005a) Trace element signature of subduction-zone fluids, melts and supercritical liquids at 120–180 km depth. Nature 437:724–727. https://doi.org/10.1038/nature03971

Kessel R, Ulmer P, Pettke T, Schmidt MW, Thompson AB (2005b) The water–basalt system at 4 to 6 GPa: phase relations and second critical endpoint in a K-free eclogite at 700 to 1400 °C. Earth Planet Sci Lett 237:873–892. https://doi.org/10.1016/j.epsl.2005.06.018

Kessel R, Fumagalli P, Pettke T (2015a) The behaviour of incompatible elements during hydrous melting of metasomatized peridotite at 4–6 GPa and 1000°C–1200°C. Lithos 236:141–155. https://doi.org/10.1016/j.lithos.2015.08.016

Kessel R, Pettke T, Fumagalli P (2015b) Melting of metasomatized peridotite at 4–6 GPa and up to 1200 °C: an experimental approach. Contrib Miner Petrol. https://doi.org/10.1007/s00410-015-1132-9

Kim N, Stebbins JF, Quartieri S, Oberti R (2007) Scandium-45 NMR of pyrope-grossular garnets: resolution of multiple scandium sites and comparison with X-ray diffraction and X-ray absorption spectroscopy. Am Miner 92:1875–1880

Klein M, Stosch H-G, Seck H, Shimizu N (2000) Experimental partitioning of high field strength and rare earth elements between clinopyroxene and garnet in andesitic to tonalitic systems. Geochim Cosmochim Acta 64:99–115

Klimm K, Blundy JD, Green TH (2008) Trace element partitioning and accessory phase saturation during H2O-saturated melting of basalt with implications for subduction zone chemical fluxes. J Petrol 49:523–553. https://doi.org/10.1093/petrology/egn001

Louvel M, Sanchez-Valle C, Malfait WJ, Testemale D, Hazemann J-L (2013) Zr complexation in high pressure fluids and silicate melts and implications for the mobilization of HFSE in subduction zones. Geochim Cosmochim Acta 104:281–299

Mottana A (1986) Crystal-chemical evaluation of garnet and omphacite microprobe analyses: its bearing on the classification of eclogites. Lithos 19:171–186

Mysen BO (2004) Element partitioning between minerals and melt, melt composition, and melt structure. Chem Geol 213:1–16

Neumann H, Mead J, Vitaliano C (1954) Trace element variation during fractional crystallization as calculated from the distribution law. Geochim Cosmochim Acta 6:90–99

O'Neill HSC, Eggins SM (2002) The effect of melt composition on trace element partitioning: an experimental investigation of the activity coefficients of FeO, NiO, CoO, MoO_2 and MoO_3 in silicate melts. Chem Geol 186:151–181

Oberti R, Quartieri S, Dalconi MC, Boscherini F, Iezzi G, Boiocchi M, Eeckhout SG (2006) Site preference and local geometry of Sc in

garnets: part I. Multifarious mechanisms in the pyrope-grossular join. Am Miner 91:1230–1239

Onuma N, Higuchi H, Wakita H, Nagasawa H (1968) Trace element partition between two pyroxenes and the host lava. Earth Planet Sci Lett 5:47–51

Papike J, Burger P, Shearer C, McCubbin F (2013) Experimental and crystal chemical study of the basalt–eclogite transition in Mars and implications for martian magmatism. Geochim Cosmochim Acta 104:358–376

Ponader CW, Brown GE Jr (1989) Rare earth elements in silicate glassmelt systems: I. Effects of composition on the coordination environments of La, Gd, and Yb. Geochim Cosmochim Acta 53:2893–2903

Prowatke S, Klemme S (2005) Effect of melt composition on the partitioning of trace elements between titanite and silicate melt. Geochim Cosmochim Acta 69:695–709

Quartieri S, Antonioli G, Geiger C, Artioli G, Lottici P (1999a) XAFS characterization of the structural site of Yb in synthetic pyrope and grossular garnets. Phys Chem Miner 26:251–256

Quartieri S, Chaboy J, Antonioli G, Geiger C (1999b) XAFS characterization of the structural site of Yb in synthetic pyrope and grossular garnets. II: XANES full multiple scattering calculations at the Yb L I-and L III-edges. Phys Chem Miner 27:88–94

Quartieri S, Boscherini F, Chaboy J, Dalconi M, Oberti R, Zanetti A (2002) Characterization of trace Nd and Ce site preference and coordination in natural melanites: a combined X-ray diffraction and high-energy XAFS study. Phys Chem Miner 29:495–502

Quartieri S, Dalconi M, Boscherini F, Oberti R, D'Acapito F (2004) Changes in the local coordination of trace rare-earth elements in garnets by high-energy XAFS: new data on dysprosium. Phys Chem Miner 31:162–167

Ryerson F, Hess P (1978) Implications of liquid-liquid distribution coefficients to mineral-liquid partitioning. Geochim Cosmochim Acta 42:921–932

Safonov O, Butvina V (2013) Interaction of model peridotite with H_2O-KCl fluid: experiment at 1.9 GPa and its implications for upper mantle metasomatism. Petrology 21:599–615

Shannon RD (1976) Revised effective ionic radii and systematic studies of interatomic distances in halides and chalcogenides. Acta Crystallogr Sect A Found Crystallogr 32:751–767

Shaw DM (1953) The camouflage principle and trace-element distribution in magmatic minerals. J Geol 61:142–151

Sun C, Liang Y (2013) The importance of crystal chemistry on REE partitioning between mantle minerals (garnet, clinopyroxene, orthopyroxene, and olivine) and basaltic melts. Chem Geol 358:23–36

Tatsumi Y, Hamilton D, Nesbitt R (1986) Chemical characteristics of fluid phase released from a subducted lithosphere and origin of arc magmas: evidence from high-pressure experiments and natural rocks. J Volcan Geotherm Res 29:293–309

Tsay A, Zajacz Z, Sanchez-Valle C (2014) Efficient mobilization and fractionation of rare-earth elements by aqueous fluids upon slab dehydration. Earth Planet Sci Lett 398:101–112

Tsay A, Zajacz Z, Ulmer P, Waelle M, Sanchez-Valle C (2016) A new experimental approach to study fluid–rock equilibria at the slab-mantle interface based on the synthetic fluid inclusion technique. Am Miner 101:2199–2209

Tsay A, Zajacz Z, Ulmer P, Sanchez-Valle C (2017) Mobility of major and trace elements in the eclogite-fluid system and element fluxes upon slab dehydration. Geochim Cosmochim Acta 198:70–91

Van Kan Parker M, Mason PR, Van Westrenen W (2011) Trace element partitioning between ilmenite, armalcolite and anhydrous silicate melt: Implications for the formation of lunar high-Ti mare basalts. Geochim Cosmochim Acta 75:4179–4193

van Westrenen W, Draper DS (2007) Quantifying garnet-melt trace element partitioning using lattice-strain theory: new crystal-chemical and thermodynamic constraints. Contrib Miner Petrol 154:717–730

van Westrenen W, Blundy J, Wood B (1999) Crystal-chemical controls on trace element partitioning between garnet and anhydrous silicate melt. Am Miner 84:838–847

van Westrenen W, Allan N, Blundy J, Purton J, Wood B (2000a) Atomistic simulation of trace element incorporation into garnets—comparison with experimental garnet-melt partitioning data. Geochim Cosmochim Acta 64:1629–1639

van Westrenen W, Blundy JD, Wood BJ (2000b) Effect of Fe^{2+} on garnet–melt trace element partitioning: experiments in FCMAS and quantification of crystal-chemical controls in natural systems. Lithos 53:189–201

van Westrenen W, Blundy JD, Wood BJ (2001) High field strength element/rare earth element fractionation during partial melting in the presence of garnet: implications for identification of mantle heterogeneities. Geochem Geophys Geosyst 2:7

van Westrenen W et al (2003) Trace element incorporation into pyrope–grossular solid solutions: an atomistic simulation study. Phys Chem Miner 30(4):217–229

Wilke M, Schmidt C, Dubrail J, Appel K, Borchert M, Kvashnina K, Manning CE (2012) Zircon solubility and zirconium complexation in $H_2O + Na_2O + SiO_2 \pm Al_2O_3$ fluids at high pressure and temperature. Earth Planet Sci Lett 349:15–25

Wood BJ, Blundy JD (2002) The effect of H_2O on crystal-melt partitioning of trace elements. Geochim Cosmochim Acta 66:3647–3656

Zou H, Reid MR (2001) Quantitative modeling of trace element fractionation during incongruent dynamic melting. Geochim Cosmochim Acta 65:153–162